Wide-field gloss scanner designed to assess appearance and condition of modern paintings

Mathieu Hébert, Pauline Hélou-de la Grandière, Yann Pozzi, Mathieu Thoury, Lionel Simonot

▶ **To cite this version:**

Mathieu Hébert, Pauline Hélou-de la Grandière, Yann Pozzi, Mathieu Thoury, Lionel Simonot. Wide-field gloss scanner designed to assess appearance and condition of modern paintings. London Imaging Meeting, IS&T, Jun 2023, London, France. hal-04144765

HAL Id: hal-04144765
https://hal.science/hal-04144765

Submitted on 28 Jun 2023

HAL is a multi-disciplinary open access archive for the deposit and dissemination of scientific research documents, whether they are published or not. The documents may come from teaching and research institutions in France or abroad, or from public or private research centers.

L'archive ouverte pluridisciplinaire **HAL**, est destinée au dépôt et à la diffusion de documents scientifiques de niveau recherche, publiés ou non, émanant des établissements d'enseignement et de recherche français ou étrangers, des laboratoires publics ou privés.

Wide-field gloss scanner designed to assess appearance and condition of modern paintings

Mathieu Hébert[1], Pauline Hélou-De la Grandière[2], Yann Pozzi[1], Mathieu Thoury[3], Lionel Simonot[4]

[1]Université Jean Monnet Saint-Etienne, CNRS, Institut d Optique Graduate School, Laboratoire Hubert Curien UMR 5516, Saint-Etienne, France; [2]Cy-Paris Université, CNRS, ministère de la Culture, Héritages : Culture/s, Patrimoine/s, Création/s UMR 9022, Cergy-Pontoise, France; [3]Université Paris-Saclay, CNRS, ministère de la Culture, UVSQ, MNHN, Institut photonique d'analyse non destructive européen des matériaux anciens UAR3461, Saint-Aubin, France; [4]Université de Poitiers, CNRS, Institut Pprime UPR 3346, Futuroscope Chasseneuil, France.

Abstract

When one seeks to characterize the appearance of art paintings, color is the visual attribute that usually focuses most attention: not only does color predominate in the reading of the pictorial work, but it is also the attribute that we best know how to evaluate scientifically, thanks to spectrophotometers or imaging systems that have become portable and affordable, and thanks to the CIE color appearance models that allow us to convert the measured physical data into quantified visual values. However, for some modern paintings, the expression of the painter relies at least as much on gloss as on color; Pierre Soulages (1919-2022) is an exemplary case. This complicates considerably the characterization of the appearance of the paintings because the scientific definition of gloss, its link with measurable light quantities and the measurement of these light quantities over a whole painting are much less established than for color. This paper reports on the knowledge, challenges and difficulties of characterizing the gloss of painted works, by outlining the track of an imaging system to achieve this.

Aspect of modern paintings: why does gloss matter?

Gloss is a visual attribute for objects that comes from the reflection by their surface of the scene around them. It often informs the observer on the smoothness or roughness of the surface, and is correlated with the reflection or scattering of light by the matter-air interface. It is an essential quality of the appearance of paintings since the glossy or matte finishing can influence the perception of colors [1]. It has evolved in the art history from the matte glue-size of High German painters to the glossy glazes of oil painting that appeared in the early Northern Renaissance. In the 20th century, gloss has become a tool of pictorial expression in itself, while some artists modulated the surface finishing in order to vary over the surface the glossiness of the painting, most often unvarnished. The "natural" gloss of the modern paintings is a real challenge to the conservators who have to restitute the gloss variations intended by the artist, thereby the fragile topologies of the surface, in order to preserve the authenticity of the artwork [2]. A decrease in gloss with time is a normal feature of the drying process of oil paintings, but it can also result from a lack of cohesion of the binder due to aging issues. Conversely, an increase in gloss of some oil paintings may be due to a chemical degradation of the binder corresponding to a softening of the material and a self-solubilization of oil. Without varnish, which was once used as a sacrificial layer, it is not possible anymore to compensate for glossiness defects. Therefore, recording the gloss, in a more quantitative way than by usual subjective written descriptions, is a crucial issue to document the appearance of an artwork at a given date and monitor it overtime. This is particularly at stake with the paintings by Pierre Soulages (1919-2022), a French painter who placed the surface reflection of light at the heart of his art.

Imaging is a well-adapted technique because it allows contactless measurements, produces data that are easy to record and easy to read by most people. However, simple photography is not enough, because the light reflections it records depend on the lighting conditions and the angle of view. While these reflections are related to the gloss of the surface, they do not represent the gloss itself and cannot be interpreted as a characteristic of the painting. For the image to represent the gloss, each pixel must contain a gloss index value calculated from a well-adapted optical acquisition, and a perceptual model linking this optical measurement with psycho-physical experiments.

In this paper, we report some of the knowledge available about gloss and the main existing techniques proposed to capture it, before presenting the principles of a new gloss acquisition system and the preliminary results obtained with it.

Gloss: definitions and measurement

Gloss sensation is produced by the human visual system by analyzing the geometrical distribution of the light reflected on the object surface. Different clues are used, in particular the consistence between the reflected light patterns and the object's shape, the viewpoint and the light source positions. In the case of a curved surface, e.g. a spherical or cylindrical object, gloss can be perceived immediately. The movement of the light patterns according to a movement of the object (translation, inclination...), of the light source or of the observer is also analyzed. Two images associated with two positions can be sufficient to discriminate radiance variations due to the object's color or to its gloss, and therefore perceive the two attributes separately.

Scientific definition for gloss as visual attribute is more recent than for color. The first one proposed by the CIE in 1970 insisted on the physical property of the material of reflecting light more or less specularly. It was then refined in 1987 by including the visual dimension: gloss is "the mode of appearance by which reflected highlights of objects are perceived as superimposed on the surface due to the directionally selective properties of that surface" [3]. As for any visual attribute, gloss assessment requires a model taking into account the response of the human visual system to the observed optical signal. This latter can be correlated to the optical properties of the surface.

The optical phenomenon underlying the glossy appearance is mainly the light reflection or scattering onto the air-matter interface (the phenomenon is also referred to as "insurface scattering", by opposition to "subsurface scattering" concerning the light that penetrates the material [4]). But light reflection is not sufficient to fully explain gloss evaluation by the human visual system, which is inherently multidimensional [5]. These first attempts of gloss assessment are mainly due to Hunter [6,7]. He subdivided gloss into several sub-attributes, in particular the specular gloss, which is the most commonly used [8]. The latter is measured with a glossmeter that gives a gloss index value in gloss units (GU), ranging on a one-dimensional scale between 0

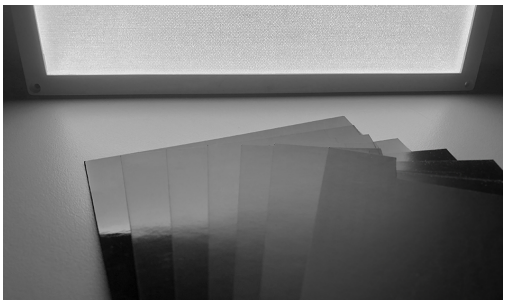

Figure 1: *Picture of the 7 black samples in the NCS gloss scale, from the glossiest (95 GU, on the left) to the most matte (2 GU, on the right).*

for matte surfaces, to a few thousands for perfect mirrors. The value 100 GU corresponds to a specular surface of reference, a smooth black glass sample having a specified refractive index. Values below 10 GU are generally considered to describe matte surfaces, and values above 70 GU describe highly glossy surfaces. The gloss index is defined as follows:

$$gloss = 100F / F_{ref} \quad (1)$$

where F and F_{ref} are the fluxes captured by the glossmeter's sensor in the specular direction with respect to the directional incident beam, being reflected by the sample, respectively by the specular reflector of reference. Between the amount of light captured by the sensor and the gloss perceived by humans, there is a non-linear transfer function that psycho-physical experiments can attempt to determine [7, 9]. Various standards specify the precise design of glossmeters and the corresponding scales in GU [10-13]. The most common devices illuminate the surface at 60°, but other incident angles are also proposed. NCS Company commercializes a calibrated gloss scale composed of seven patches, displayed in Figure 1, whose respective gloss indices in GU are 95 (Full gloss), 75 (Glossy), 50 (Semi-glossy), 30 (Satin), 12 (semi-matte), 6 (matte), 2 (Full matte).

Because of its simple and rigid configuration, the glossmeter is not able to render all the kinds of shine that humans are able to perceive. Moreover, it has three major drawbacks which prevent its use on pictorial masterpieces: 1) measurements are in contact with the object of study, which is suitable for rigid and common surfaces, but becomes impossible with soft, fragile or precious surfaces; 2) the area analyzed is usually of the order of cm², which is very large for analyzing heterogeneous surfaces in gloss, 3) the gloss index values are highly distorted when the shape of the surface is not flat, e.g., wavy, ridged, or textured like the leather surfaces shown in Figure 2. In this figure are specified the gloss index of the NCS patch having the closest apparent gloss, and the gloss index measured at 60° with the X-rite YG268 TRI-angle glossmeter (average between measurements in 6 different positions on the surface). The discrepancy between the two values is very significant.

Beyond the specular gloss measured by a glossmeter, it is now well accepted that the most appropriate radiometric function to account for the sensation of gloss is the Bidirectional Reflectance Distribution Function (BRDF) [14, 15], a function that describes the way the surface reflects light angularly according to the direction of illumination. In order to account for the change of BRDF in the different positions of a heterogenous surface, the BRDF concept is extended to the Spatially Varying Bidirectional Reflectance Distribution Function (svBRDF) [16] or the Bidirectional Texture Function (BTF). Various solutions based on imaging systems have been proposed to measure svBRDFs or BTFs where either the camera, the sample or the source is moved during the acquisition of the pictures. In most systems, the camera

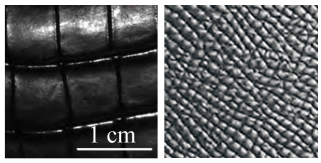

Specular gloss measured:	6.5 GU	31 GU
NCS tile visually the closest:	30 GU	75 GU

Figure 2*: Pictures of two non-flat surfaces (leather pieces) and gloss index values given by a glossmeter, compared to the gloss index of the NCS scale patch that appears visually the closest in terms of gloss.*

is fixed to prevent registration of the different pictures, while either the sample is tilted under a fixed source [17] or the light source is rotated around a fixed sample (the rotating source being more often a set of point sources distributed over space and turned on sequentially) [18-22]. Even though the first prototypes of these systems were rather heavy, more portable setups are being developed [23] that can be used in situ in museums. Most often, computer vision algorithms based on approximate BRDF models are used to extract topology, light scattering properties and appearance attributes of the surface. The system that we present hereinafter relies on similar principles, with a fixed wide-field camera and a light source that moves linearly.

Gloss scanner: principles

Our imaging system is contactless and allows wide-field observation. A fixed camera is placed at a distance z_c from the surface of the painting (see Figure 3). Its height from the floor, h_c, and orientation, denoted by a vector $\mathbf{N_C}$, are adjusted in order to target the wanted area of the painting, the field of view being centered around a point V of the surface. A point source (in practice, a small LED) is mounted on a rail, placed parallel to the surface at a distance z_s from it and at a height z_c from the floor, equal to the height of point V. While the source moves linearly along the rail, the camera captures pictures corresponding to different equally-spaced positions of the source.

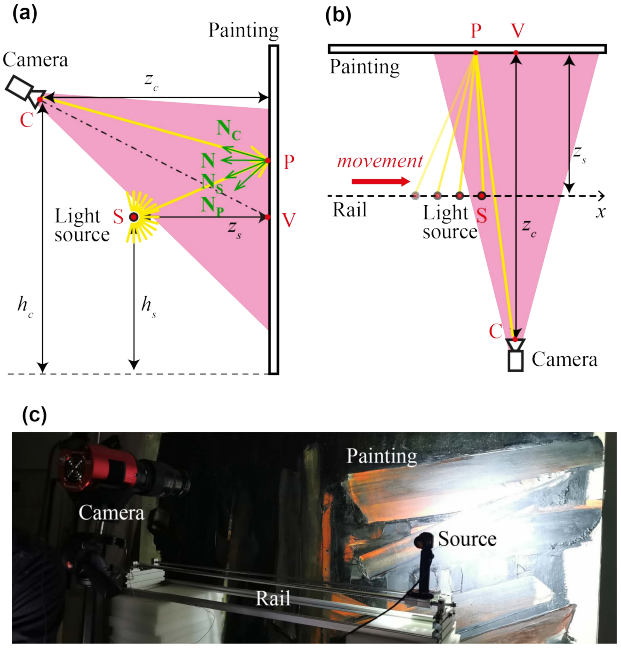

Figure 3: *Side view (a) and top view (b) schematic of the gloss scanner comprising a point source S moving along a line parallel to the surface, a camera whose field of view is centered on a point V of the surface. (c) Prototype of the gloss scanner in use on a painting by Pierre Soulages in Les Abattoirs, Musée – Frac Occitanie Toulouse, France.*

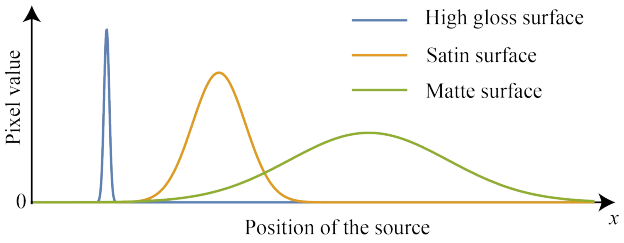

Figure 4: *Typical variations of the grey level of a pixel of the camera according to the position of the light source during its movement, in the case of a glossy surface, a satin surface or a matte surface.*

In all the pictures captured sequentially, the light received by a given pixel (*i*,*j*) is issued from the same small area on the surface, around a point denoted P. The amount of light received by the sensor in this pixel is a radiance *L*. If the surface is not flat, this area around P has a certain normal vector $\mathbf{N_P}$ that is not parallel to the normal **N** of the mean plane of the surface. For a given position *x* of the light source S on the rail, the irradiance *E*(*x*) of the small area around P depends on the local angle of incidence of light, $\arccos(\mathbf{N_S}\cdot\mathbf{N_P})$, the length *d* = PS, and the intensity of the source *I* in the direction $\mathbf{N_S}$ which can be determined beforehand (the angular intensity diagram of the source is assumed to be rotationally symmetric around **N**). Hence, if $\mathbf{N_P}$, $\mathbf{N_S}$, $I(\mathbf{N_S})$, *d* are known, it is possible to relate the grey level in pixel (*i*, *j*), proportional to *L*, and the BRDF f_r of the surface around P:

$$f_r(\mathbf{N_S},\mathbf{N_P},\mathbf{N_C},\mathrm{P}) = \frac{L}{E(x)} = \frac{Ld^2}{I(\mathbf{N_S})\langle\mathbf{N_S}\cdot\mathbf{N_P}\rangle} \qquad (2)$$

With the different source positions, we obtain the BRDF values attached to the corresponding angles of incidence.

When using this system with a very glossy surface (e.g., a mirror), it is expected that for a given source position, the recorded image has only a few pixels illuminated, those corresponding to the image of the source reflected by the surface. The value of other pixels is zero. When the source moves to another position, other few pixels are illuminated. In the successive pictures acquired during the movement of the source, a given pixel remains black if it has not met the reflection of the source; or it is black, then becomes suddenly bright, then suddenly dark again. The set of pixels that can be bright belongs to a narrow band at the center of the field of view of the camera.

With a rougher surface, thus with satin appearance, the transition between black and bright values in a given pixel is more gradual, and the set of pixels that can be illuminated belongs to a larger band. The signal acquired in a pixel during the acquisition process is similar to the curves plotted in Figure 4.

Test of the gloss scanner with NCS gloss scale patches

The gloss scanner was tested with a board covered by four patches of the NCS gloss scale, with respective gloss values 95, 75, 50 and 30. The source is a LED, and the camera a ZWO ASI2600MM-Pro 16 bytes grey level camera, with 26 million pixels (6248 × 4176). The source was placed at 50 cm from the surface, and the camera at 1 m.

The successive images acquired during the movement of the source are combined into a maximum radiance map, shown in Figure 5.a, in which each pixel is set to its maximum value in the different images. For the sake of illustration, we have selected in each patch one position on the surface, highlighted by a colored square, and plotted in Figure 5.b the grey level in this position as a function of the source position *x*. On the glossiest patch, as expected, the value of the pixels that have received light

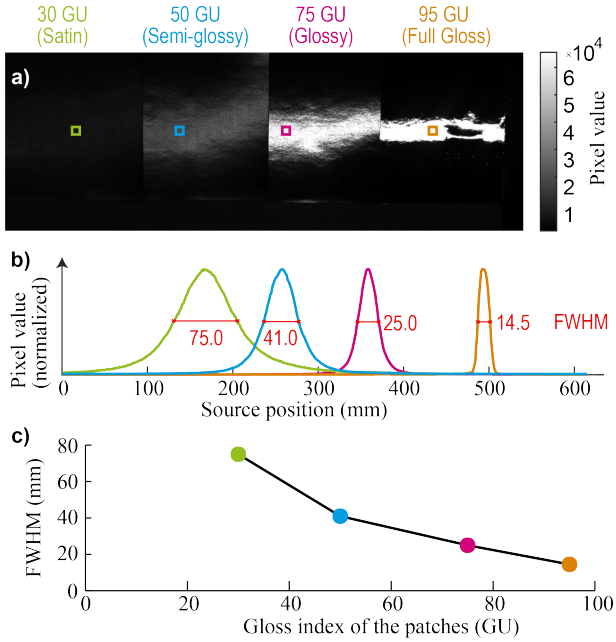

Figure 5: *a) Maximum radiance map of a surface composed of four patches of the NCS gloss scale. b) normalized curves showing the variations of the grey level of four pixels in the image, one per patch of the gloss scale, indicated by the colored squares on the maximum radiance map. The FWHM of each curve is indicated in red. c) FWHM of the curves vs nominal gloss index value of the patches.*

at a certain time during the scanning process varies abruptly. These pixels, easily identifiable thanks to the bright points in the map, are mainly located into a band at the center of the field of view of the camera; the band is not regular due to some local waviness of the patch. The pixels whose value remains close to zero correspond to areas that have not reflected any light towards the camera due to the direction of their local normal. Gloss cannot be assessed in these areas; however, it is possible to change the height of the rail supporting the source, and operate a new scan that will provide gloss information in a new set of areas.

For the other patches, which are less glossy, the grey level of the pixels in this band vary in a more gradual way; the maximum values are lower than for the glossiest patch. The band where pixels are non-zero is larger: its width increases as the gloss index of the patch decreases. In a very first approach, in order to quantify gloss with a numbered score, one can consider the FWHM of the lobes, which is specified near each curve. The relationship between the FWHM and the nominal gloss index attached with each patch, plotted in Figure 5.c, is not linear but bijective. Deeper analysis of the shape of the lobes is intended in order to improve the relevance of the gloss scores.

Acquisitions on a painting

The gloss scanner was used to study a painting by Pierre Soulages, at Les Abattoirs, Musée – Frac Occitanie in Toulouse, France. The painting (*Peinture 202 x 125 cm, 15 décembre 1959*) is an oil on canvas, non-figurative, where black layers cover a lighter underlayer (with red, grey, white shades). The artist, by stretching and tearing the impasto in the wet, made the colored underlayer appear with shades of color and gloss. The work was initially conceived without varnish, but a synthetic varnish had been applied before its acquisition by the Musée des Abattoirs in 1994, then removed some twenty years ago. Today, after these multiple vicissitudes on the surface, changes in appearance are observed: the conservator interprets them either as "augmented matte", when the work seems more matte than the contemporary works of the artist, or as "excessive gloss", in areas where the

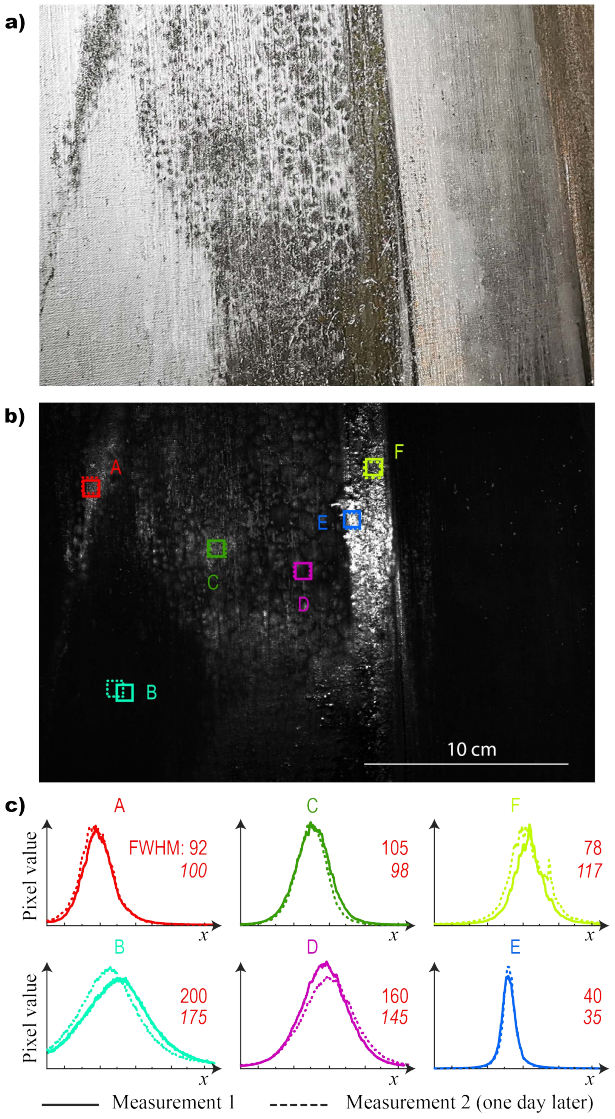

Figure 6: *a) Color picture under grazing lighting of the painting area studied. b) Corresponding maximum radiance map, and positions of the six manually selected windows. c) Variations of the average pixel values in these windows as functions of the position of the source. The solid lines correspond to a first measurement, the dashed lines to a second measurement made one day later.*

binder medium suffers from chemical transformation in progress linked to an ongoing self-solubilization. The localization and qualification of these zones represent a major issue for the conservation of the work since the excesses of gloss indicate chemical degradations in progress. And beyond the detection of degradations, it is also important for art historians and for the respect of the artist's intent to record and archive the global appearance of the work.

The camera and LED as well as their distance to the surface were the same as for the test with the NCS gloss scale. Various areas of the painting were studied. Figure 6 shows one of these areas in which various levels of gloss are present and the corresponding maximum radiance map. The measurements were done twice, one day apart, the painting having been moved and the setup dismantled then reassembled between the two measurements. The position of the camera and rail were approximately reproduced, but not exactly, which results in slightly different maximum radiance maps (only the first map is displayed). As for the NCS gloss scale, by way of illustration, we manually selected 6 positions on the first map, featured by colored square in solid line. Point E belongs to the glossiest area, which is depicted by a bright value in the maximum radiance map and by a narrow lobe in the curve function of the source position. Point B is in a more matte area. We tried to locate the corresponding positions in the second map, despite the slight misregistration of the two maps; they are indicated by dotted squares. For each position, an average grey level has been calculated over a window of a 10×10 px. The average grey level is plotted as a function of the source position for each position and each measurement; the scales in ordinate are different for the six graphs but in each of them, the two curves are plotted on the same scale. The FWHM is mentioned in red, roman font for the first measurement, and italic font for the second measurement. Even though an automated registration method would have been suitable for a better comparison, and therefore a better assessment of the reproducibility of the method, the difference between the two measurements is rather small for a first prototype. The deviation of the two FWHM for each position is around 10%, except for position F, located in a very textured area, where it approaches 50%. Deeper analysis of the curves attached to individual pixels in this area, and averaging over a smaller window would be instructive to understand this level of deviation. Future work will intend to improve the analysis of the characteristics of these lobes and establish a more precise relationship with the perceived gloss, either by benchmarking the curve shapes to those obtained from a standard gloss scale, or performing psycho-physics experiments.

Conclusions and perspectives

Modern painters such as Pierre Soulages have used gloss appearance for their artistic expression, with a glossiness ranging from matte to very glossy. It is crucial for conservators to be able to record a quantitative and reliable assessment of such an attribute appearance at a given time, in order to allow comparisons with the appearance of other similar works, or with the same work at later moments. This new type of information can also be a base of interdisciplinary exchange on how and when such imaging strategy can assist conservators during their restoration actions. This paper introduces an imaging system based on a fixed wide-field camera and a moving point source that moves linearly. The gray values taken by each pixel of the camera during the source travel forms an information-rich signal, which can be related to a portion of BRDF through a radiometric calculation, or can simply be compared to reference signals acquired on flat standard surfaces whose gloss index is measured by a glossmeter in a standardized perceptual scale. The algorithms for processing these signals still need to be refined and better correlated with psycho-physics experiments, but the simple FWHM of signals acquired on patches of the NCS gloss scale already shows a good bijective correlation with the gloss index values (in GU). The principle outlined here can be extended to a source moving in 2D, i.e., in a plane parallel to the study surface. The grey level curves in each pixel would also become 2D. It can also be combined with topographic and colorimetric measurements. The measurements carried out in situ in the reserves of a museum show the operationality of this portable and contactless bench for the gloss characterization of works of art.

Acknowledgements

This work has been founded by the “Nuit Noiroes” project, supported by the PIA4 Excellences UP-Squares program of the University of Poitiers, France. The authors would like to thank Thierry Lépine, and Anthony Cazier from Institut d’Optique Graduate School, Emmanuel Kim, Serge Cohen, and Marouane Ben Jelloul from Ipanema for their technical contribution and interesting discussions at different steps of this research.

References

1 A. Giumlia-Mair, C. Albertson, G. Boschian, G. Giachi, P. Iacomussi, P. Pallecchi, G. Rossi, A. N. Shugar and S. Stock, ”Surface characterization techniques in the study and conservation of art and archaeological artefacts: a review”, Materials Technology, 25:5, p. 245-261 (2010).

2 P. Iacomussi, M. Radis and G. Rossi, ”Goniometric and colorimetric properties of paints and varnish”, Proc. SPIE, Measuring, Modeling, and Reproducing Material Appearance, p.201 1 214 (2015).

3 ASTM, E284-05a – Standard termninology of appearance. ASTM International, West Conshohocken (2005).

4 A.Ferrero, J. R. Frisvad, L. Simonot, P. Santafé, A. Schirmacher, J. Campos, M. Hébert, “Fundamental scattering quantities for the determination of reflectance and transmittance,” Opt. Express 29, 219–23 (2021).

5 F. B. Leloup, G. Obein, M.R. Pointer, P. Hanselaer, “Toward the soft metrology of surface gloss: A review,” Color Res. Appl. 39, 559–570 (2014).

6 R.S. Hunter “Methods of determining gloss,” NBS Research paper 958 (1937),

7 R.S. Hunter, R.W. Harold *The Measurement of Appearance*, 2nd Ed., Wiley, New-York (1987).

8 R. Sève, J.-F. Decarreau “Appareils usuels de mesure du brillant”, in Simonot, L., Quand la matière diffuse la lumière, Presse des Mines, Paris, 91–103 (2019, in French)

9 CIE (1995) *Evaluation of the attribute of appearance called gloss*, CIE technical report.

10 ASTM, D523-14 – *Standard Test Method for Specular Gloss*, ASTM International, West Conshohocken (2014)

11 ISO, 2813 – *Paint and varnishes – Determination of gloss value at 20°, 60° and 85°, ISO/TC35/SC9*, International Organization for Standardization, Geneva (2014).

12 TAPPI, *Specular gloss of paper and paperboard at 75 degrees*, TAPPI/ANSI Test method T 480 om-20.

13 TAPPI, *Specular gloss of paper and paperboard at 20 degrees*, TAPPI/ ANSI Test method T 653 om-07.

14 G. Obein, *Caractérisation optique et visuelle du brillant,* PhD dissertation, Conservatoire National des Arts et Métiers, Paris, France (2003, in French).

15 ASTM, E430-19 – Standard Test Methods for Measurement of Gloss of High-Gloss Surfaces by Abridged Goniophotometry, ASTM International, West Conshohocken (2019).

16 B. Raymond, G. Guennebaud, P. Barla. “Multi-scale rendering of scratched materials using a structured SV-BRDF model.” ACM Trans. Graph. 35, 4, Article 57 (2016).

17 Y. Arteaga, C. Boust, A. Dequier, J.Y. Hardeberg, "Image-based goniometric appearance characterisation of bronze patinas" IS&T 29th Color Imaging Conference (CIC), pg 294 – 299 (2021).

18 Y. Arteaga, C. Boust, A. Dequier, J.Y. Hardeberg, "HDR multispectral imaging-based BRDF measurement using flexible robot arm system" IS&T 30th Color Imaging Conference (CIC), 75-80 (2022).

19 A. Lucat, *Acquisition opto-numérique de vêtements asiatiques anciens*, PhD dissertation, Université de Bordeaux. *In French* (2020).

20 M. Aittala, T. Weyrich, J. Lehtinen et al. “Two-shot svbrdf capture for stationary materials,” ACM Trans. Graph., 34, 110–1 (2015).

21 J. Riviere, P. Peers, A. Ghosh, “Mobile surface reflectometry,” ACM SIGGRAPH 2014 Posters. Association for Computing Machinery (2014).

22 C. Schwartz, R. Sarlette, M. Weinmann, R. Klein. “DOME II: A parallelized BTF acquisition system,” Eurographics (2013).

23 C. Schmitt, S. Donne, G. Riegler, V. Koltun et al. “On joint estimation of pose, geometry and svbrdf from a handheld scanner,” Proceedings of the IEEE/CVF Conference on Computer Vision and Pattern Recognition, pg 3493–3503 (2020).